

# Cholesterol is important in control of EGF receptor kinase activity but EGF receptors are not concentrated in caveolae

Tove Ringerike<sup>1</sup>, Frøydis D. Blystad<sup>1</sup>, Finn O. Levy<sup>2</sup>, Inger H. Madshus<sup>1</sup> and Espen Stang<sup>1,\*</sup>

<sup>1</sup>Institute of Pathology, University of Oslo, Rikshospitalet University Hospital, N-0027 Oslo, Norway

<sup>2</sup>MSD Cardiovascular Research Center, Rikshospitalet University Hospital and Department of Pharmacology, University of Oslo, N-0316 Oslo, Norway

\*Author for correspondence (e-mail: espenst@ulrik.uio.no)

Accepted 19 December 2001

Journal of Cell Science 115, 1331-1340 (2002) © The Company of Biologists Ltd

## Summary

We have investigated the localization and function of the epidermal growth factor receptor (EGFR) in normal cells, in cholesterol-depleted cells and in cholesterol enriched cells. Using immunoelectron microscopy we find that the EGFR is randomly distributed at the plasma membrane and not enriched in caveolae. Binding of EGF at 4°C does not change the localization of EGFR, and by immunoelectron microscopy we find that only small amounts of bound EGF localize to caveolae. However, upon patching of lipid rafts, we find that a significant amount of

the EGFR is localized within rafts. Depletion of the plasma membrane cholesterol causes increased binding of EGF, increased dimerization of the EGFR, and hyperphosphorylation of the EGFR. Addition of cholesterol was found to reduce EGF binding and reduce EGF-induced EGFR activation. Our results suggest that the plasma membrane cholesterol content directly controls EGFR activation.

Key words: Caveolae, Caveolin, Cholesterol, EGFR, Rafts

## Introduction

Based on detergent-free membrane fractionation experiments as much as 40-60% of the total pool of EGFR at the plasma membrane has been reported to localize to caveolae in nonstimulated cells not overexpressing the EGFR (Mineo et al., 1999). In A431 cells, which overexpress the EGFR, similar detergent-free fractionation experiments have shown that the majority of the EGFR is localized within caveolin enriched low-buoyant density membrane domains (Couet et al., 1997; Pike and Miller, 1998; Waugh et al., 1999). However, whereas caveolin is restricted to detergent insoluble membrane fractions, the EGFR in A431 cells was found to be detergent soluble (Pike and Casey, 1996; Waugh et al., 1999), and Waugh et al. concluded that the EGFR is localized within low-buoyant density, noncaveolar membrane domains. Different results have been reported regarding localization of EGFR upon ligand-induced activation. Although some studies conclude that activated EGFR remains in caveolin-positive membrane fractions (Couet et al., 1997; Waugh et al., 1999), Mineo et al. found that activated EGFR relocates to caveolin-negative membranes even at 4°C (Mineo et al., 1999).

It should be noted that caveolin-enriched membrane domains isolated by fractionation contain both caveolae and lipid rafts in general. Lipid rafts are membrane domains enriched in cholesterol and sphingolipids. Although caveolae also have such characteristics, lipid rafts also exist in the plasma membrane outside morphologically defined caveolae, as well as in cells not expressing caveolin (for reviews, see Brown and London, 1998; Kurzchalia and Parton, 1999; Simons and Ikonen, 2000; Simons and Toomre, 2000).

Electron microscopy (EM) is required to discover whether the EGFR is localized within morphologically identifiable caveolae. In the classical studies by the groups of Cohen (Haigler et al., 1979) and Hopkins (Hopkins et al., 1985; Miller et al., 1986), the EGFR was localized either directly using anti-EGFR-coated colloidal gold (Hopkins et al., 1985; Miller et al., 1986) or indirectly by the localization of bound EGF-ferritin complexes (Haigler et al., 1979). These studies showed that in nonstimulated cells the EGFR is more or less randomly distributed at the plasma membrane and not concentrated within any specific morphologically identifiable microdomain. Incubation with EGF at 4°C did not seem to change the random distribution of EGFR (Hopkins et al., 1985; Miller et al., 1986; Torrisi et al., 1999). However, upon chase at 37°C, Hopkins et al., reported that the EGFR relocated into noncoated plasma membrane invaginations resembling caveolae (Hopkins et al., 1985). Again, other studies showed that the EGFR relocates into clathrin-coated pits (Ringerike et al., 1998; Stang et al., 2000; Torrisi et al., 1999).

The importance of rafts in signal transduction has been demonstrated indirectly in several studies where the composition of rafts has been modulated by changes in the plasma membrane cholesterol content (reviewed by Incardona and Eaton, 2000; Kurzchalia and Parton, 1999; Simons and Toomre, 2000). Cholesterol depletion has previously been shown to cause activation of Erk, and further incubation with EGF enhanced the effect, causing hyperactivation of Erk (Furuchi and Anderson, 1998). This could suggest that cholesterol depletion directly affects EGF-induced activation of the EGFR; however, this was not addressed in the published

study (Furuchi and Anderson, 1998). Cholesterol depletion will change the biophysical properties of the plasma membrane, making it more fluid (reviewed by Burger et al., 2000; Yeagle, 1985). Studies of EGFR activation upon reconstitution of EGFR into liposomes have shown that the lipid composition influences EGFR kinase activity. Introduction of cholesterol into the liposome membrane resulted in decreased kinase activity, thus indicating that membrane fluidity affects the tyrosine kinase activity of reconstituted EGFR (Ge et al., 2001).

In the present work we have studied the plasma membrane localization of EGFR with respect to caveolae and lipid rafts and characterized the role of cholesterol in control of EGF binding, EGFR dimerization and phosphorylation of the EGFR. To avoid complicating effects of endocytosis of the EGFR, all experiments have been performed at 4°C. Our results show that although only a small percentage of EGFR is localized within caveolae, the cholesterol content of the plasma membrane is critical for control of EGFR activity. This

suggests that localization to lipid rafts might control the EGFR and, as support for this, we find that a significant number of EGFR colocalize with the raft-localized GPI-anchored protein, placental alkaline phosphatase (PLAP), upon antibody-induced patching.

## Materials and Methods

### Materials

Human recombinant EGF was from Bachem Feinchemikalien AG (Budendorf, Switzerland). All reagents were from Sigma Chemical Co. (St Louis, MO), unless otherwise noted.

### Antibodies

Antibodies used were rabbit anti-caveolin 1 (Transduction Laboratories, Lexington, KY), mouse anti-EGFR (Santa Cruz Biotechnology, Santa Cruz, CA; Neomarkers, Lab Vision, Fremont, CA), sheep anti-EGFR (Gibco BRL Life Technologies, Gaithersburg, MD), mouse anti-phosphorylated EGFR (PY1173, Upstate Biotechnology, Lake Placid, NY), mouse anti-human PLAP (DAKO, Carpinteria, CA), rabbit anti-human transferrin receptor (HybriDomus, Nota Bene Scientific, Hellebaek, Denmark), rabbit anti-mouse IgG (Cappel, ICN Biomedicals, Costa Mesa, CA). Rabbit anti-sheep IgG, alkaline phosphatase-conjugated donkey anti-sheep IgG, peroxidase-conjugated donkey anti-mouse IgG and peroxidase-conjugated donkey anti-sheep IgG were all from Jackson ImmunoResearch Laboratories, West Grove, PA.

### Cell culture and treatment

The human laryngeal carcinoma cell line HEP-2 was grown in

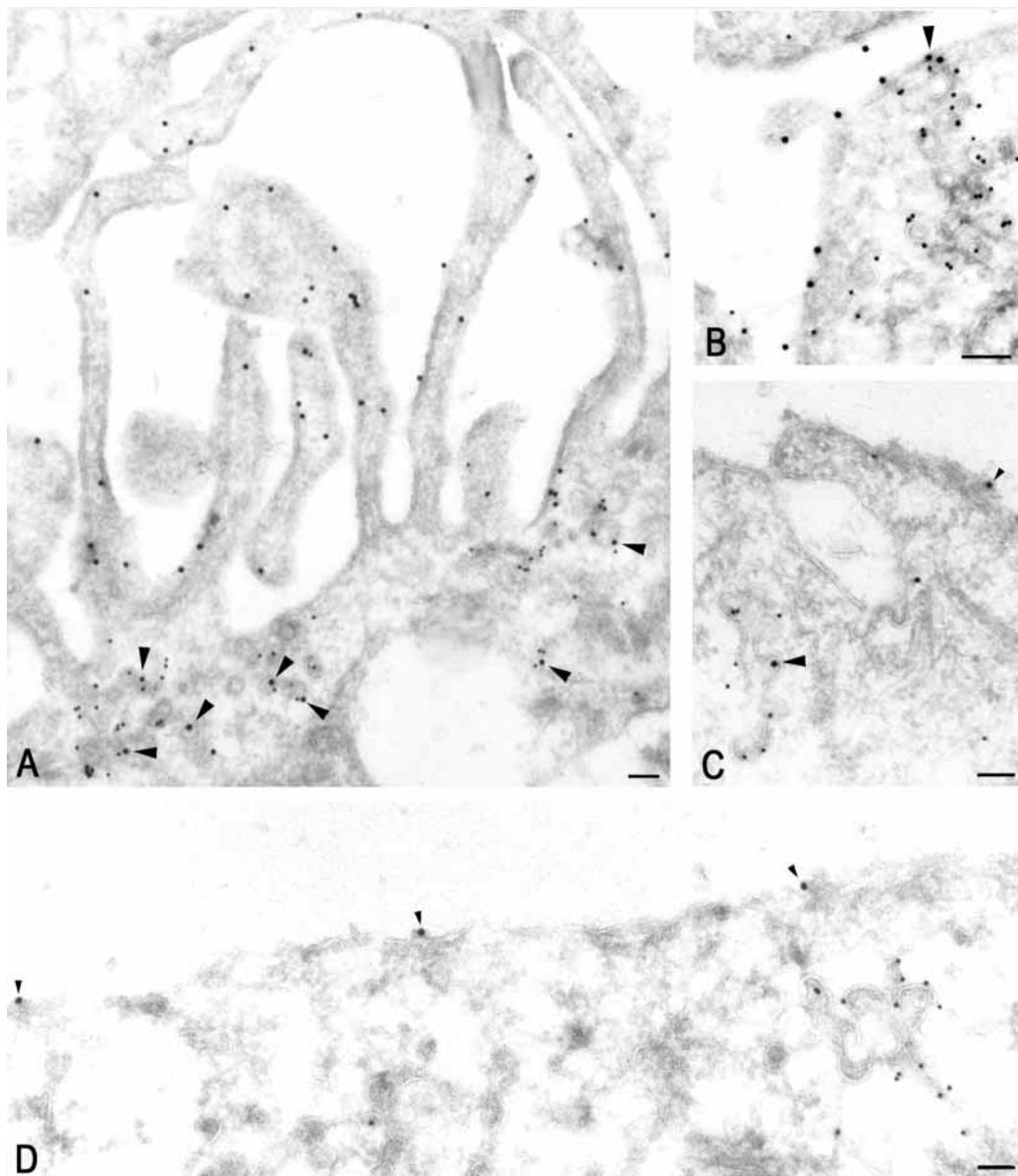
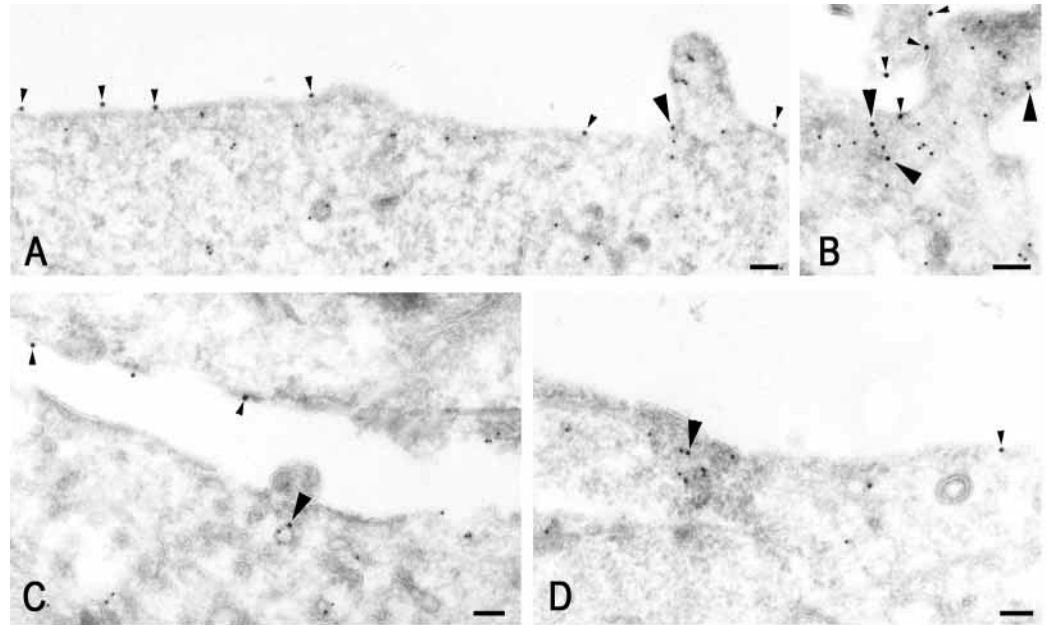


**Fig. 1.** Immuno-EM shows that EGFR is localized mainly outside caveolae. Ultrathin cryosections of nonstimulated cells were double labeled to localize EGFR (large gold particles) and caveolin (small gold particles). A431 cells (A,B) showed strong labeling for EGFR but very limited colocalization of EGFR (large arrowheads) with caveolin in caveolae. In HEP-2 cells (C,D) EGFR labeling was less intense but, as in A431 cells, EGFR labeling was mainly at smooth noninvaginated areas of the plasma membrane (small arrowheads) with only small amounts colocalizing (large arrowheads) with caveolin in caveolae. Bars, 100 nm.

**Fig. 2.** Immuno-EM shows that binding of EGF mainly occurs outside caveolae. Ultrathin cryosections of cells incubated with EGF (10 nM) for 15 minutes on ice were double-labeled to localize bound EGF (large gold particles) and caveolin (small gold particles). In both A431 cells (A,B) and HEp-2 cells (C,D) bound EGF was found at smooth noninvaginated areas of the plasma membrane (small arrowheads), and only small amounts colocalized with caveolin in caveolae (large arrowheads). Bars, 100 nm.



Dulbecco's modified Eagle's medium (3.7 g/l sodium bicarbonate) (BioWhittaker, Walkersville, MD) containing 2 mM L-glutamine (BioWhittaker) and 1× penicillin-streptomycin-fungizone mixture (17-745, BioWhittaker) supplemented with 5% (v/v) fetal bovine serum (FBS) (BioWhittaker). The human epidermal carcinoma cell line A431 was grown in the same medium, but with 10% (v/v) FBS. HEp-2 cells were plated at a density of 15,000 cells/cm<sup>2</sup> and A431 cells at a density of 25,000 cells/cm<sup>2</sup> 48 hours prior to experiments. EGF (0.1, 1.0 or 10 nM) was added to cells in minimal essential medium (MEM) (Gibco BRL) without HCO<sub>3</sub><sup>-</sup> and with 0.1% (w/v) bovine serum albumin (BSA) for 15 minutes on ice. The cells were then washed three times with ice-cold PBS (137 mM NaCl, 2.7 mM KCl, 1 mM Na<sub>2</sub>HPO<sub>4</sub> and 2 mM NaH<sub>2</sub>PO<sub>4</sub>) to remove unbound ligand. To deplete cholesterol from the plasma membrane, cells were incubated with 10 mM methyl-β-cyclodextrin (MβCD) in MEM, for 15 minutes at 37°C, or with 1 μg/ml U18666A (3-β-(2-diethylaminoethoxy)-androstene-HCl) (BioMol Research Laboratories, Plymouth Meeting, PA) for 48 hours in DMEM. To add cholesterol to the plasma membrane, the cells were incubated with MEM containing MβCD-cholesterol (water-soluble cholesterol, ~0.4 mg cholesterol/ml) for 30 minutes at 37°C.

#### Western blotting

Cells were lysed in lysis buffer (10 mM Tris-HCl (pH 6.8), 5 mM EDTA, 50 mM NaF, 30 mM sodium pyrophosphate, 1% Triton X-100, 1 mM Na<sub>3</sub>VO<sub>4</sub> and 1 mM phenyl methyl sulphonyl fluoride (PMSF)) on ice for 10 minutes and subjected to western blotting, as described (Ringerike et al., 1998). The reactive proteins were detected using an enhanced chemiluminescence method (ECL, Amersham Pharmacia Biotech, Piscataway, NJ). For quantitation of band intensity, proteins were electrotransferred to polyvinylidene difluoride membranes (Hybond-P, Amersham Pharmacia Biotech) upon SDS-PAGE. The membranes were incubated with sheep anti-EGFR antibodies before incubation with alkaline phosphatase-conjugated anti-sheep IgG. Immunobinding was detected by the enhanced chemifluorescence method (ECF, Amersham Pharmacia Biotech), and the chemifluorescence was measured by a phosphorfluorImager (Molecular Imager FX, Bio-Rad, Hercules, CA).

#### Analysis of <sup>125</sup>I-EGF binding

HEp-2 cells plated in 24- or 48-well cell culture plates at half the normal density were preincubated with or without 10 mM MβCD, 1

μg/ml U18666A or 0.4 mg/ml water-soluble cholesterol, as described above. Binding of <sup>125</sup>I-EGF was performed and data analysed essentially as previously described (Ringerike et al., 1998). To measure the total number of EGF binding sites, binding was performed for 15 minutes on ice with a saturating concentration (8 nM) of <sup>125</sup>I-EGF (Amersham Pharmacia Biotech) in the absence (total binding) or presence (nonspecific binding) of 150 nM unlabeled EGF. The cells were then washed in ice-cold PBS, lysed in 1 M NaOH, and bound radioactivity was measured.

#### Crosslinking of the EGFR

Cells were washed with ice-cold PBS before incubation on ice for 30 minutes with the nonpermeable crosslinking reagent bis(sulfosuccinimidyl) suberate (BS<sup>3</sup>) (3 mM in PBS) (Pierce, Rockford, IL). In all experiments, a freshly prepared solution of BS<sup>3</sup> was used. The crosslinking reaction was terminated by adding glycine (1 M) to a final concentration of 250 mM and further incubation on ice for 5 minutes. The cells were washed in PBS, scraped loose and transferred to test tubes followed by centrifugation at 420 g for 5 minutes at 4°C. The cell pellets were lysed on ice in lysis buffer containing 250 mM glycine. The lysates were homogenized using QIAshredder™ (Qiagen, Valencia, CA) before being subjected to SDS-PAGE using 4-15% gradient gels (Bio-Rad) and western blotting with quantitation of band intensity as described above.

#### Biotinylation of the EGFR

HEp-2 cells, nontreated or preincubated with U18666A, MβCD, or water-soluble cholesterol, as described above, were washed three times in PBS containing 1 mM CaCl<sub>2</sub> and 0.5 mM MgCl<sub>2</sub> (CaMg-PBS) before incubation with 1.8 mM EZ-Link™ Sulfo-NHS-LC-Biotin (Pierce, Rockford, IL) for 1 hour on ice. To stop the reaction, cells were washed three times with CaMg-PBS and incubated with 20 mM glycine in CaMg-PBS for 10 minutes on ice. Cells were washed with CaMg-PBS and lysed in immunoprecipitation buffer (PBS containing 10 mM EDTA, 1% (v/v) Triton X-100, 10 mM NaF, 200 U/ml aprotinin (Fluka Chemie AG, Buchs, Switzerland), 1 mM PMSF, 1 mM N-ethylmaleimide and 1 mM Na<sub>3</sub>VO<sub>4</sub>) on ice 20 minutes before the lysates were centrifuged at 20,000 g for 15 minutes at 4°C. Anti-EGFR antibodies bound to protein G-coupled Sepharose beads (Amersham Pharmacia Biotech) were added to the supernatant

fraction, and immunoprecipitation was performed at 4°C for 1 hour. The immunoprecipitate was washed and subjected to SDS-PAGE and western blotting. Biotinylated EGFR was detected by use of alkaline phosphatase conjugated streptavidine (DAKO Corporation).

#### Fluorescence microscopy

Cells were plated on 12 mm coverslips (MENZEL-GLÄSER®, Germany) in 24-well microtiter plates, two to three days prior to experiments. Cells were fixed in 4% (w/v) paraformaldehyde in Soerensen's buffer (0.162 M Na<sub>2</sub>HPO<sub>4</sub>, 0.038 M NaH<sub>2</sub>PO<sub>4</sub>) for 20 minutes at room temperature and washed three times in cytoskeleton buffer (137 mM NaCl, 5 mM KCl, 1.1 mM Na<sub>2</sub>HPO<sub>4</sub>·H<sub>2</sub>O, 0.4 mM KH<sub>2</sub>PO<sub>4</sub>, 5.5 mM glucose, 4 mM NaHCO<sub>3</sub>, 10 mM MES, 2 mM EGTA, 2 mM MgCl<sub>2</sub>). To localize cholesterol, coverslips were

incubated with 50 µg/ml filipin in PBS containing 0.2% BSA and 0.2% gelatin (Bio-Rad) for 30 minutes at room temperature, washed and mounted using DAKO fluorescent mounting medium with 15 mM NaN<sub>3</sub> (DAKO). To visualize the filipin labeling, cells were viewed using a Leitz DM RXE microscope equipped with a UV filter and an F-view digital camera.

#### Immunolectron microscopy (immuno-EM)

To patch PLAP, HEp-2 cells were incubated with mouse anti-PLAP antibodies, followed by rabbit anti-mouse IgG and, finally, 5 nm protein A-gold (purchased from G. Posthuma, Utrecht, The Netherlands), each for 30 minutes on ice. Cells with patched PLAP, or otherwise preincubated as described in legends to figures, were fixed with paraformaldehyde (4% w/v) and glutaraldehyde (0.1% w/v) in Soerensen's phosphate buffer and processed for cryosectioning and immunolabeling (Griffiths et al., 1984). Bound antibodies were visualized using protein A-gold. When the primary antibody was mouse IgG or sheep IgG, incubation with rabbit anti-mouse IgG or rabbit anti-sheep IgG, respectively, was used as an intermediate reagent between the primary antibody and protein A-gold. The sections were examined using a Philips CM 120 electron microscope. To estimate the number of EGFR at the plasma membrane, EGFR labeling density was quantitated. The number of gold particles representing EGFR labeling at the plasma membrane of randomly chosen cells was counted, the length of the plasma membrane was measured and the number of gold particles per unit membrane length was calculated.

#### Results

The EGFR is partly localized to lipid rafts and not concentrated in caveolae

The distribution of the EGFR at the plasma membrane was investigated using immuno-EM. Thawed cryosections of nonstimulated A431 cells and HEp-2 cells were double-labeled using antibodies recognizing either the extracellular or the intracellular domain of the EGFR and anti-caveolin 1 antibodies. Since A431 cells strongly overexpress the EGFR, labeling intensity was much stronger in A431 cells compared with HEp-2 cells. However, the distribution was similar in both cell types. Regardless of the antibody used, EGFR labeling was found all along the plasma membrane with only small amounts localized to caveolae (Fig. 1). Quantitation showed that approximately 7% of the total number of EGFR at the plasma membrane was within caveolae in A431 cells, while approximately 5% localized to caveolae in HEp-2 cells. The rest of

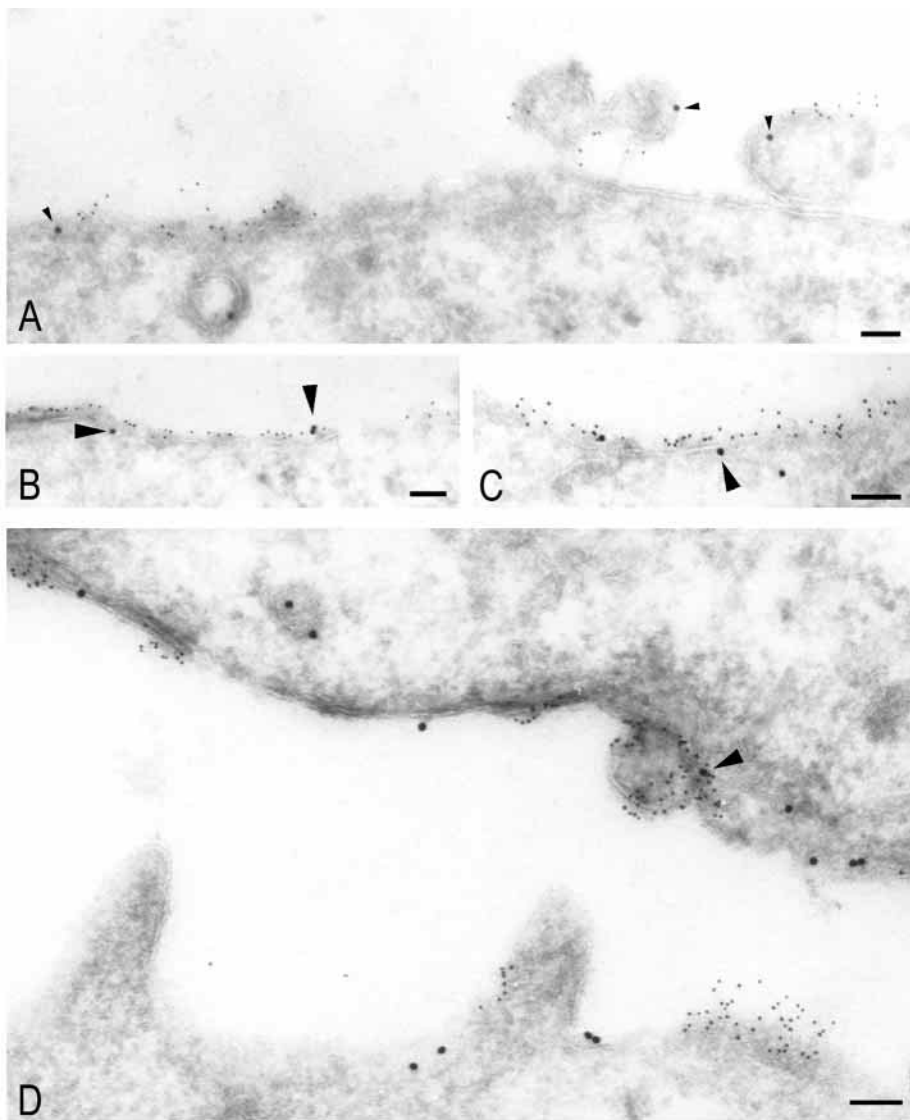
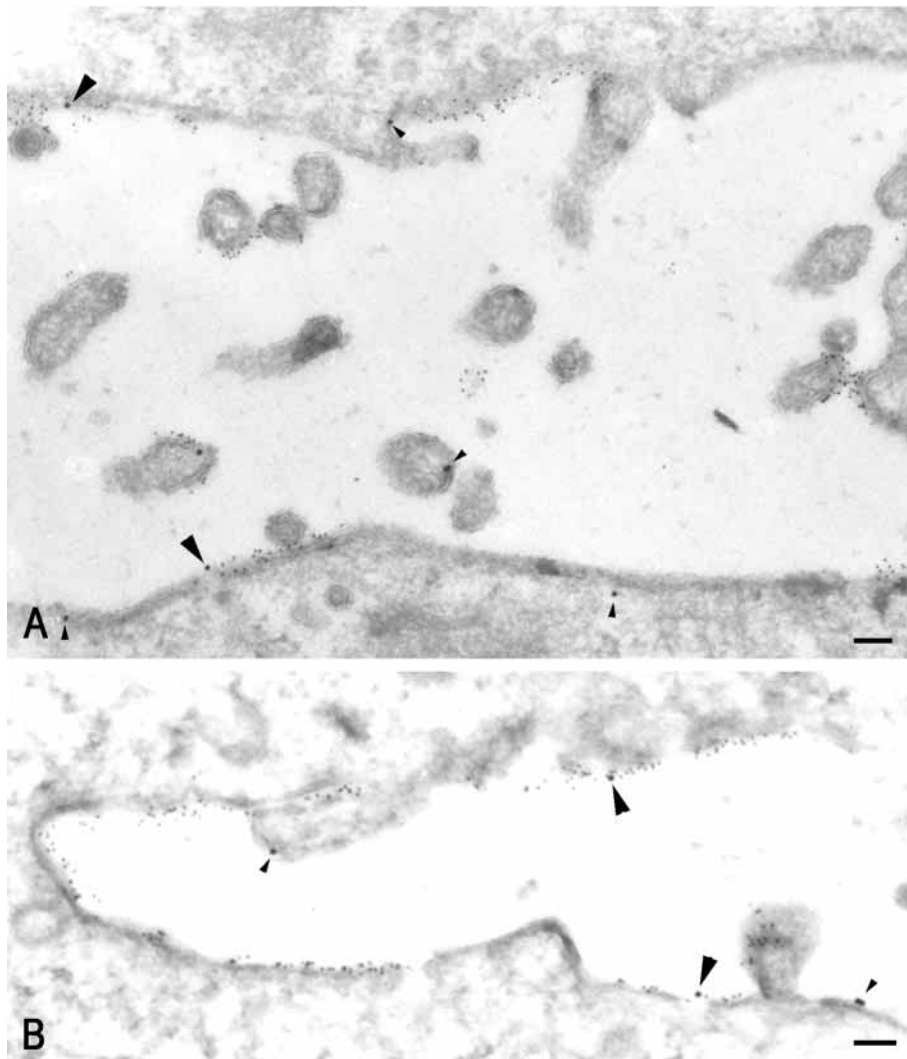


**Fig. 3.** Immuno-EM shows that whereas EGFR in nonstimulated cells localizes both within and outside rafts, TfR localizes outside rafts. To patch PLAP, HEp-2 cells were incubated with mouse anti-PLAP antibodies, followed by rabbit anti-mouse IgG and finally 5 nm protein A-gold. Each incubation was for 30 minutes on ice. Ultrathin cryosections of HEp-2 cells with patched PLAP (small gold particles) were labeled (large gold particles) to detect localization of EGFR (A-C) or TfR (D). Labeling for EGFR was found both outside (small arrowheads in A) and within (large arrowheads in B,C) PLAP patches. Labeling for TfR was mainly found outside PLAP patches. Bars, 100 nm.

**Fig. 4.** Immuno-EM shows that binding of EGF occurs to EGFR both inside and outside rafts. PLAP was patched as described in Fig. 3, except that EGF (10 nM) was added together with 5 nm protein A-gold. Labeling for EGFR (A) showed that incubation with EGF on ice did not change the localization of the EGFR. Labeling for EGFR was found both outside (small arrowheads) and within (large arrowheads) rafts. Labeling for EGF (B) showed that EGF bound to EGFR both outside (small arrowheads) and within (large arrowheads) rafts. Bars, 100 nm.



the labeling was found outside caveolae and with no accumulation in clathrin-coated pits.

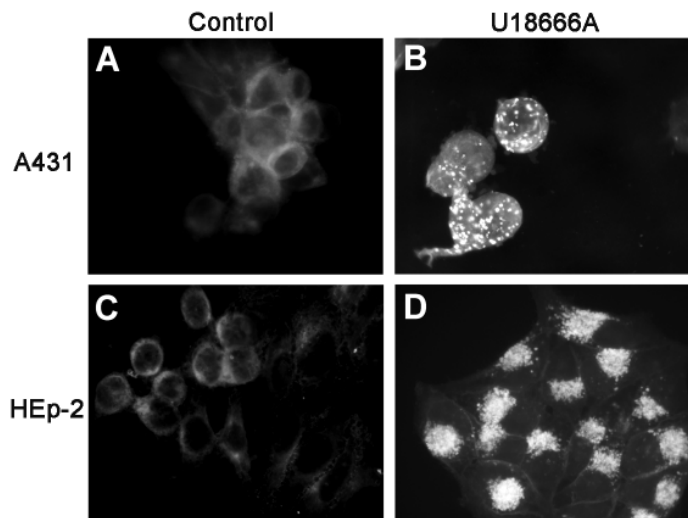
We also localized the EGFR in cells incubated with EGF at 4°C. Double labeling of cells incubated with 10 nM EGF on ice for 15 minutes showed no change in the number of EGFR localized to caveolae compared with the number in nonstimulated cells (data not shown). In the same cells, we also studied the plasma membrane distribution of bound EGF to investigate whether EGFR localized to caveolae bound EGF with higher efficiency than did EGFR outside caveolae. These experiments demonstrated the same distribution of EGF labeling as for EGFR with 6% localizing to caveolae in A431 cells and 5% in HEP-2 cells (Fig. 2).

Most previous reports on caveolar localization of EGFR have been based on fractionation experiments. Since fractionation techniques will not separate rafts in general from caveolae, we also studied the localization of EGFR to lipid rafts in general. As rafts, with the exception of caveolae, cannot be identified by morphological criteria, we identified rafts indirectly after patching of raft-associated molecules. Rafts in HEP-2 cells were visualized by patching the GPI-anchored protein PLAP (Harder et al., 1998). Following incubation with mouse anti-PLAP, the bound antibodies were crosslinked using rabbit anti-mouse antibodies followed by 5 nm protein A-gold. To see whether binding of EGF influences the possible raft-localization of the EGFR, in some experiments EGF was included during the protein A-gold incubation. The antibody-induced crosslinking of PLAP resulted in clearly identifiable patched areas at the plasma membrane. To determine EGFR localization with regard to rafts, sections were labeled using antibodies to the EGFR or, as a control, anti-transferrin receptor (TfR) antibodies (Fig. 3). The labeling demonstrated that the EGFR localized both within and outside rafts. Quantitation of EGFR within anti-PLAP patched rafts showed that about 40% of EGFR localizing to the plasma membrane is within rafts in nonstimulated cells. Similar quantitation of TfR labeling showed that only about 6% of TfR at the plasma membrane colocalized with patched PLAP, confirming that anti-PLAP-induced patches represent rafts and not just

unspecific trapping of plasma membrane components. Labeling of cells incubated with EGF during the final incubation with protein A-gold showed that ligand binding on ice did not affect the EGFR localization. Both EGFR and bound EGF showed the same quantitative distribution as the EGFR in nonstimulated cells (Fig. 4).

#### Cholesterol depletion increases the number of EGFR at the plasma membrane and causes EGFR hyperactivation

Our present immuno-EM results, as well as several previous studies, indicate that a substantial amount of the EGFR is localized within rafts; rafts are cholesterol-rich membrane domains. To study whether cholesterol directly affects EGFR activation, we used two established methods to deplete the plasma membrane of cholesterol. M $\beta$ CD extracts cholesterol (Kilsdonk et al., 1995; Klein et al., 1995), whereas U18666A causes a redistribution of cholesterol from the plasma membrane to late endosomes (Liscum and Klasek, 1998). The effect of U18666A was initially investigated by fluorescence microscopy. Filipin staining demonstrated that cholesterol was redistributed from the plasma membrane to intracellular



vesicles (Fig. 5). To make sure that the different drugs had the expected effect on clathrin-coated pits and caveolae, drug-treated cells were prepared for immuno-EM. Both cholesterol-depleting drugs caused flattening of clathrin-coated pits, and invaginated caveolae were no longer observed (data not shown).

The effect of cholesterol depletion on expression and activation of EGFR was examined by western blotting, by using antibodies recognizing either all EGFR or the EGFR phosphorylated on tyrosine 1173 (PY1173). Both cholesterol-depleting drugs caused an increase in EGFR tyrosine phosphorylation (Fig. 6). In A431 cells increased phosphorylation of the EGFR could be seen even in the absence

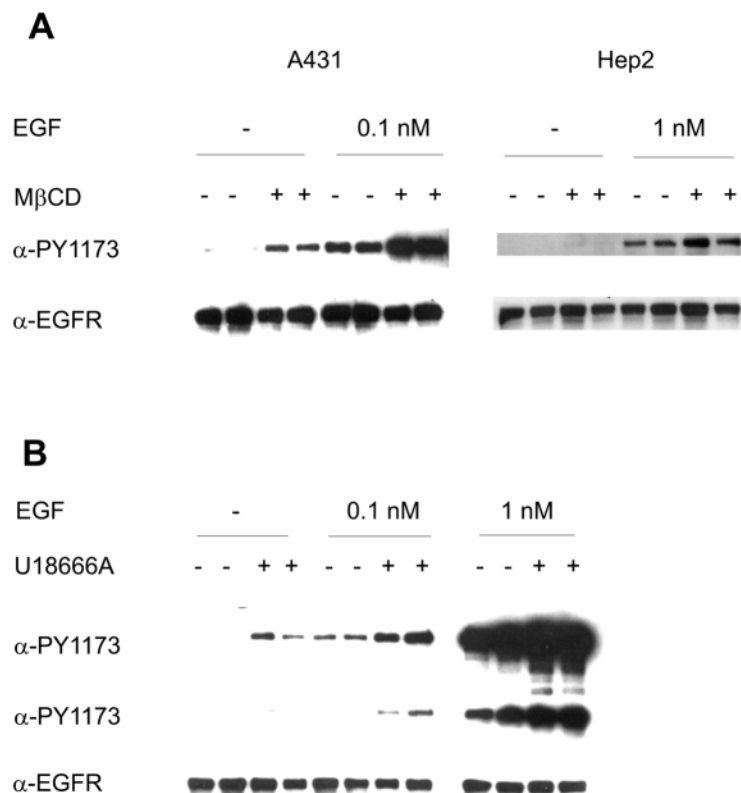


**Fig. 5.** Incubation with U18666A causes intracellular accumulation of cholesterol. A431 cells (A,B) and Hep-2 cells (C,D) were incubated with or without 1  $\mu$ g/ml U18666A for 48 hours prior to fixation. Cholesterol was labeled using filipin, as described in Materials and Methods. In untreated cells (A,C) filipin labeled mainly the plasma membrane. Upon treatment with U18666A (B,D) filipin labeling revealed accumulation of cholesterol in intracellular vesicles.

of added EGF, while the effect of cholesterol depletion was observed only upon incubation with EGF in Hep-2 cells. The different EGFR expression levels in the two cell lines most likely explain this difference. Additionally, A431 cells are known to produce growth factors that activate the EGFR in an autocrine fashion (Van de Vijver et al., 1991). To examine whether the increased activation of EGFR induced by treatment with M $\beta$ CD or U18666A was a direct effect of changes in the plasma membrane cholesterol content, we incubated cells with water-soluble cholesterol to increase the cholesterol content of the plasma membrane. Incubation with water-soluble cholesterol was observed to result in diminished EGF-induced phosphorylation of the EGFR (Fig. 7).

The EGFR usually exists in two affinity states. To examine whether cholesterol depletion increased EGFR phosphorylation by increasing the number of high affinity EGFR, we measured binding of iodinated EGF to cells and performed Scatchard analysis. When cholesterol-depleted cells and cells enriched in cholesterol were compared with untreated cells, we found no difference in the fraction of high-affinity binding sites (data not shown). However, saturation binding experiments demonstrated that specific binding of EGF was increased upon cholesterol depletion and decreased in cells enriched in cholesterol (Fig. 8).

Binding of EGF involves dimerization of the EGFR, and it was recently suggested that the predominant mechanism for dimerization is the formation of a complex of one EGF molecule and an EGFR dimer, followed by the direct arrest of a second EGF molecule (Sako et al., 2000). By this mechanism, increases in EGF-induced EGFR dimerization can cause increased EGF binding without necessarily affecting binding affinity. To examine whether changes in plasma membrane cholesterol content caused changes in EGFR dimerization, we took advantage of a chemical crosslinking reagent previously used for this purpose (Johannessen et al., 2001; Sorkin and Carpenter, 1991).

**Fig. 6.** Cholesterol depletion induces increased tyrosine phosphorylation of the EGFR. (A) A431 cells and Hep-2 cells were pre-incubated with (+) or without (-) 10 mM M $\beta$ CD for 15 minutes at 37°C, cooled with ice-cold PBS and further incubated with or without EGF in MEM with or without 10 mM M $\beta$ CD for 15 minutes on ice. Whereas A431 cells were incubated with 0.1 nM EGF, Hep-2 cells were incubated with 1 nM EGF to achieve detectable ligand-induced phosphorylation. The cells were lysed and subjected to SDS-PAGE and western blotting, using antibodies to EGFR and PY1173. (B) A431 cells were pre-incubated with (+) or without (-) 1  $\mu$ g/ml U18666A for 48 hours prior to incubation with or without EGF (0.1 or 1.0 nM) for 15 minutes on ice. To demonstrate differences in EGFR tyrosine phosphorylation (PY1173) upon incubation with 1 nM EGF, two different exposures of the blot are shown.

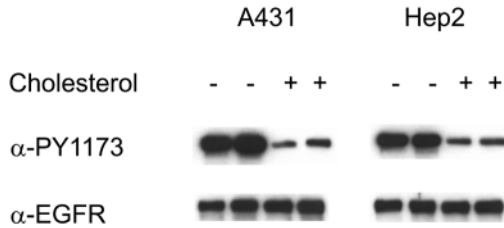


**Fig. 7.** Incubation with water-soluble cholesterol decreases tyrosine phosphorylation of the EGFR. A431 cells and HEP-2 cells were preincubated with (+) or without (-) 0.4 mg/ml water-soluble cholesterol for 30 minutes at 37°C, cooled with ice-cold PBS, and further incubated with 10 nM EGF in the absence or presence of cholesterol for 15 minutes on ice. Blotting with antibody to PY1173 revealed a large decrease in EGFR phosphorylation in cells incubated with water-soluble cholesterol. However, blotting with antibody to EGFR showed equal amounts of EGFR in cell lysates irrespective of addition of cholesterol.

Control cells, M $\beta$ CD-treated cells and cells enriched in cholesterol were upon incubation with or without EGF for 15 minutes on ice incubated with the membrane-impermeable crosslinking reagent BS<sup>3</sup>, and the cell lysates were subsequently subjected to western blotting with antibodies to EGFR. As demonstrated in Fig. 9, cholesterol depletion caused increased EGF-induced EGFR dimerization, whereas addition of water-soluble cholesterol inhibited EGF-induced EGFR dimerization. The increased dimerization in cholesterol-depleted cells was 21%.

Neither cholesterol depletion, nor incubation with water soluble cholesterol, affected the total level of EGFR (Figs 6, 7). However, a possible explanation for the observed changes in EGF binding, EGFR activation and EGFR dimerization could be altered EGFR distribution with more EGFR localizing to the plasma membrane. To investigate this possibility, the amount of EGFR localized at the plasma membrane was measured by biotinylation of the plasma membrane. By calculating the fraction of biotinylated EGFR, we found that cholesterol depletion indeed caused a change in EGFR distribution. Even though the total level of EGFR expression was unaltered, more EGFR became biotinylated, demonstrating that more EGFR localized to the plasma membrane (Fig. 10). The increased number of EGFR at the plasma membrane upon cholesterol depletion was confirmed by immuno-EM. Although labeling density varied from cell to cell within the same specimen, quantitation showed that labeling density for EGFR at the plasma membrane on average increased by approximately 25% upon both M $\beta$ CD and U18666A treatment of HEP-2 cells.

## Discussion

The plasma membrane is not uniform, but can be divided into different microdomains. Whereas some microdomains, such as clathrin-coated pits, are morphologically identifiable, others can be identified only upon colocalization with domain-specific

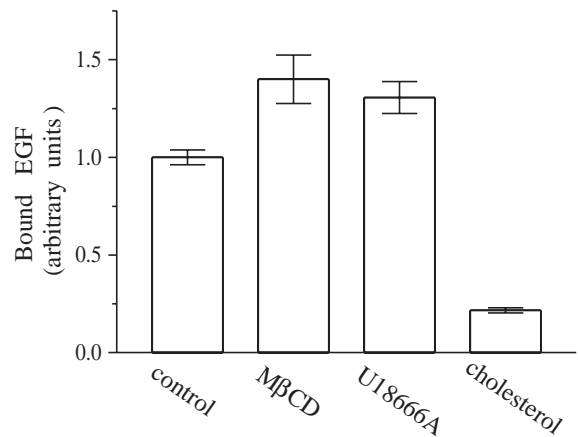


**Fig. 8.** Cholesterol depletion and incubation with water-soluble cholesterol has opposite effects on EGF binding. Untreated HEP-2 cells (control) and HEP-2 cells preincubated with either 10 mM M $\beta$ CD for 15 minutes (M $\beta$ CD), 1  $\mu$ g/ml U18666A for 48 hours (U18666A), or 0.4 mg/ml water-soluble cholesterol for 30 minutes (cholesterol) were incubated with <sup>125</sup>I-EGF for 15 minutes on ice. Bound <sup>125</sup>I-EGF was measured as described in Materials and Methods. EGF bound to control cells was set to be 1 (approx.  $1 \times 10^5$  binding sites/cell). The figure shows one representative experiment of three measured in triplicate (means  $\pm$  s.e.m.).

marker molecules. Caveolae are microdomains originally identified morphologically as small noncoated invaginations of the plasma membrane. The formation of caveolae depends on expression of caveolin and, since the plasma membrane contains different noncoated invaginations, caveolae can be identified only by labeling for caveolin. Some confusion exists with respect to the relationship between caveolae and lipid rafts [see raft nomenclature (Simons and Toomre, 2000)]. This is partly due to difficulties in isolating pure caveolae and to the various methods used for this purpose. Initially, subcellular fractionation upon Triton X-100 extraction at 4°C was used. Such fractionation allows the isolation of detergent-resistant membranes [DRMs; also called DIGs (detergent-insoluble glycolipid-enriched membranes) or GEMs (glycolipid-enriched membranes)]. Although caveolin is enriched in such fractions, DRMs can be isolated from cells not expressing caveolin (Fra

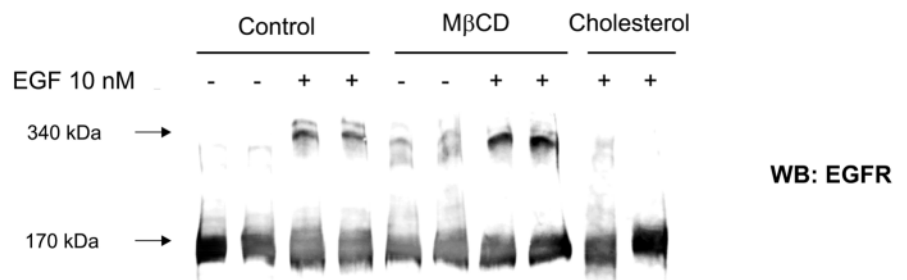


**Fig. 9.** Incubation with M $\beta$ CD or water-soluble cholesterol has opposite effects on EGFR dimerization. HEP-2 cells were preincubated either with (+) or without (-) 10 mM M $\beta$ CD for 15 minutes, or with 0.4 mg/ml water-soluble cholesterol for 30 minutes at 37°C. The cells were subsequently incubated with or without 10 nM EGF for 15 minutes on ice. The EGFR was crosslinked by the crosslinker BS<sup>3</sup>, before cell lysis, SDS-PAGE and western blotting, using an antibody to EGFR, as described in Materials and Methods. Bands at 170 kDa represent EGFR monomers, whereas bands at 340 kDa represent EGFR dimers.

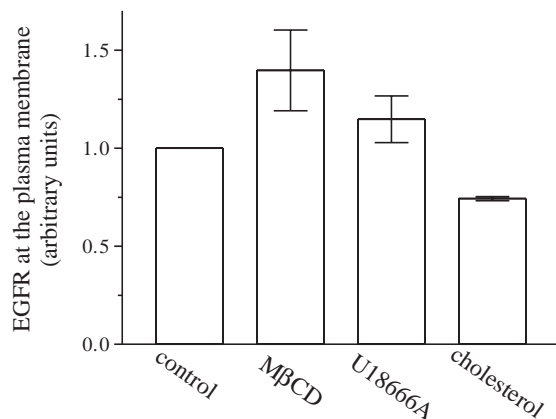


**Fig. 10.** Cholesterol depletion affects the cellular distribution of EGFR. Untreated HEP-2 cells (control) or HEP-2 cells preincubated with 10 mM MβCD for 15 minutes (MβCD), 1 μg/ml U18666A for 48 hours (U18666A), or 0.4 mg/ml water-soluble cholesterol for 30 minutes (cholesterol), were biotinylated as described in Materials and Methods. The fraction of biotinylated EGFR (plasma-membrane-localized EGFR) was calculated. Biotinylated EGFR in control cells was set to be 1. The figure shows pooled data from three independent experiments (means±s.e.m.).

et al., 1995) and therefore can probably represent a number of different rafts. Detergent-free methods have been developed to isolate low-buoyant density fractions enriched in caveolin. However, like DRMs, low-buoyant density fractions contain rafts without caveolin. Because of this, some investigators have changed their definition of caveolae or caveolae-related domains to include caveolin-negative membranes (Anderson, 1998; Smart et al., 1999). However, as morphologically identifiable caveolae clearly represent specialized microdomains, we believe it is important to restrict the definition of caveolae to caveolin-positive plasma membrane invaginations.

In the present study we have used immuno-EM to characterize the plasma membrane distribution of the EGFR. Based on the colocalization between EGFR and caveolin 1 we show that only a limited number of EGFR resides within caveolae. As noncoated invaginations, most likely representing caveolae, previously have been shown to occupy approximately 7% of the plasma membrane in A431 cells (Parton, 1994), our results could indicate that the EGFR is randomly distributed at the plasma membrane. Our results are in conflict with those of several fractionation studies, where the authors have concluded that the EGFR is enriched in caveolae, but in agreement with prior EM studies (Haigler et al., 1979; Hopkins et al., 1985; Miller et al., 1986; Torrisi et al., 1999). Based on fractionation experiments, as much as 40-60% of EGFR has been reported to localize to caveolae (Mineo et al., 1999). These numbers correspond well with the number of EGFR we find colocalized with patched PLAP, indicating that this represents the number of EGFR localizing to rafts in general and not only to caveolae.

Different results with respect to the impact of ligand binding on localization of EGFR have been reported. Whereas some authors conclude that activated EGFR remains in caveolin-positive membrane fractions (Couet et al., 1997; Waugh et al., 1999), Mineo et al. found that activated EGFR relocates to caveolin-negative membranes even at 4°C (Mineo et al., 1999).

Our results showed no change in EGFR distribution upon incubation with EGF at 4°C. Previously we have shown that as much as 50% of EGFR activated at 4°C relocated to coated pits upon chase at 37°C (Stang et al., 2000), but whether this represents a relocation with respect to lipid rafts is unclear. In fact, the flattening of clathrin-coated pits upon cholesterol depletion illustrates the importance of cholesterol for the integrity and function of clathrin-coated pits (Rodal et al., 1999).

Labeling for EGF showed the same distribution as found for EGFR. This indicates that, at high ligand concentrations, ligand binds to EGFR with the same efficiency within and outside rafts. Attempts to localize high-affinity EGFR by incubation with limiting concentrations of EGF failed because of inefficient labeling intensity for EGF. The mechanisms determining high versus low affinity binding of ligand are still unclear. The finding that the percentage of EGFR localizing to caveolae corresponds to the percentage of high-affinity EGFR in the cells examined, could suggest that caveolar localization is important for high-affinity binding. However, considering the finding that conditions disrupting the organization of caveolae had no effect on the fraction of high-affinity EGFR, this is very unlikely.

Changes in the cholesterol content of the plasma membrane had significant effects on the amount of EGF bound to cells as well as on dimerization and activation of the EGFR. However, whether these effects are direct or indirect consequences of changes in cholesterol content is unclear. A possible explanation for the increase in binding of EGF and for the increase in dimerization and activation of the EGFR could be the altered sub-cellular distribution of the EGFR and increased number of EGFR at the plasma membrane upon cholesterol depletion. The increase in plasma membrane EGFR is most likely due to inhibited endocytosis of the EGFR. Although the major endocytosis of EGFR is ligand induced, EGFR is also constitutively endocytosed and recycled in a ligand-independent manner (Herbst et al., 1994). As cholesterol depletion inhibits endocytosis but, as shown for the transferrin receptor, not recycling (Subtil et al., 1999), the number of EGFR available for binding of EGF will increase as an indirect consequence of cholesterol depletion. However, the effect on clathrin-dependent endocytosis does not explain the inhibitory effects found after incubation with water-soluble cholesterol. This suggests that cholesterol also controls the EGFR in a direct fashion. Upon cholesterol depletion, the fluidity of the plasma membrane increases with increased possibility of lateral movement of the EGFR. Increased lateral mobility will probably increase the possibility of EGF-induced EGFR dimerization and thereby EGFR activation.

How EGF binds to monomeric versus dimeric EGFR is an unresolved issue. Our results showed that dimeric EGFR could be detected only upon incubation with EGF. This could support the theory that dimerization is induced by the initial binding of EGF to monomeric EGFR and that eventually dimers are formed. However, whether dimerization involves binding of one or more EGF molecules is unclear. Sako et al. recently claimed that single molecule tracking revealed that the predominant mechanism of dimerization involves the formation of a complex of one EGF molecule and one EGFR dimer, followed by the direct arrest of a second EGF molecule (Sako et al., 2000). This would suggest that dimerization occurs before binding of the

second EGF molecule. This sequence of events could explain how changes in cholesterol content and ensuing changes in membrane fluidity might affect EGF binding. Increased EGF-induced EGFR dimerization due to increased lateral mobility will also increase the chance for binding of a second EGF molecule. Increased cholesterol content of the plasma membrane will have the opposite effect on fluidity and thereby, in theory, the opposite effect on EGFR dimerization and total EGF binding. As activation of the EGFR depends on dimerization, such a model for EGF binding will explain not only the observed changes in EGF binding and EGFR dimerization, but also the changes in EGFR activation.

It is important to realize that cholesterol depletion could inhibit interaction between the EGFR and other molecules involved in control of EGFR activation. The ganglioside GM3 is known to modulate EGFR activity (Bremer et al., 1986; Meuillet et al., 1999; Meuillet et al., 2000) either directly (Rebbaa et al., 1996) or via a phosphatase (Suarez Pestana et al., 1997). Changes in GM3 content do not affect EGF binding but, whereas GM3 depletion increases EGFR autophosphorylation, addition of GM3 decreases EGFR autophosphorylation (Meuillet et al., 1999; Meuillet et al., 2000). Membranes enriched in GM3, also known as the 'glycosphingolipid signaling domain' or the 'glycosignaling domain' can, like lipid rafts, be isolated as a low density detergent insoluble membrane fraction. However, as reported for the EGFR, GM3-containing membranes can be separated from caveolin-containing membranes (Iwabuchi et al., 1998). The GM3-positive membranes contain less cholesterol than caveolin-positive membranes and rafts in general (Iwabuchi et al., 1998). However, as incubation with M $\beta$ CD, and most likely also incubation with U18666A, depletes cholesterol not only from rafts (Ilangumaran and Hoessli, 1998), we cannot exclude the possibility that disorganization of GM3-positive glycosignaling domains can cause at least some of the observed effects on EGFR activation.

In conclusion, contrary to results based on subcellular fractionation, immuno-EM studies show that only small amounts of EGFR localize to caveolae. However, a significant amount of EGFR was found to colocalize with patched PLAP. This demonstrates that a significant amount of EGFR localizes to rafts. Cholesterol was found to be important in control of EGFR activation and its depletion probably has multiple effects on EGFR localization and activation. Whether cholesterol controls the EGFR directly or only indirectly, by regulating endocytosis through clathrin-coated pits and thereby affecting the level of EGFR at the plasma membrane, is still unclear.

We thank Rob Parton for helpful discussions. This work has been supported in part by Medinnova, Novo Nordisk Foundation, Anders Jahre's Foundation for the Promotion of Science, Blix Legacy and Bruun's Legacy. T.R. was supported by a fellowship from The Norwegian Research Council. E.S. was supported by a research fellowship from the Norwegian Cancer Society.

## References

- Anderson, R. G.** (1998). The caveolae membrane system. *Annu. Rev. Biochem.* **67**, 199-225.
- Bremer, E. G., Schlessinger, J. and Hakomori, S.** (1986). Ganglioside-mediated modulation of cell growth. Specific effects of GM3 on tyrosine phosphorylation of the epidermal growth factor receptor. *J. Biol. Chem.* **261**, 2434-2440.
- Brown, D. A. and London, E.** (1998). Functions of lipid rafts in biological membranes. *Annu. Rev. Cell Dev. Biol.* **14**, 111-136.
- Burger, K., Gimpl, G. and Fahrenholz, F.** (2000). Regulation of receptor function by cholesterol. *Cell Mol. Life Sci.* **57**, 1577-1592.
- Couet, J., Sargiacomo, M. and Lisanti, M. P.** (1997). Interaction of a receptor tyrosine kinase, EGF-R, with caveolins. Caveolin binding negatively regulates tyrosine and serine/threonine kinase activities. *J. Biol. Chem.* **272**, 30429-30438.
- Fra, A. M., Williamson, E., Simons, K. and Parton, R. G.** (1995). De novo formation of caveolae in lymphocytes by expression of VIP21-caveolin. *Proc. Natl. Acad. Sci. USA* **92**, 8655-8659.
- Furuchi, T. and Anderson, R. G.** (1998). Cholesterol depletion of caveolae causes hyperactivation of extracellular signal-related kinase (ERK). *J. Biol. Chem.* **273**, 21099-21104.
- Ge, G., Wu, J. and Lin, Q.** (2001). Effect of membrane fluidity on tyrosine kinase activity of reconstituted epidermal growth factor receptor. *Biochem. Biophys. Res. Commun.* **282**, 511-514.
- Griffiths, G., McDowall, A., Back, R. and Dubochet, J.** (1984). On the preparation of cryosections for immunocytochemistry. *J. Ultrastruct. Res.* **89**, 65-78.
- Haigler, H. T., McKanna, J. A. and Cohen, S.** (1979). Direct visualization of the binding and internalization of a ferritin conjugate of epidermal growth factor in human carcinoma cells A-431. *J. Cell Biol.* **81**, 382-395.
- Harder, T., Scheiffele, P., Verkade, P. and Simons, K.** (1998). Lipid domain structure of the plasma membrane revealed by patching of membrane components. *J. Cell Biol.* **141**, 929-942.
- Herbst, J. J., Opresko, L. K., Walsh, B. J., Lauffenburger, D. A. and Wiley, H. S.** (1994). Regulation of postendocytic trafficking of the epidermal growth factor receptor through endosomal retention. *J. Biol. Chem.* **269**, 12865-12873.
- Hopkins, C. R., Miller, K. and Beardmore, J. M.** (1985). Receptor-mediated endocytosis of transferrin and epidermal growth factor receptors: a comparison of constitutive and ligand-induced uptake. *J. Cell Sci. Suppl.* **3**, 173-186.
- Ilangumaran, S. and Hoessli, D. C.** (1998). Effects of cholesterol depletion by cyclodextrin on the sphingolipid microdomains of the plasma membrane. *Biochem. J.* **335**, 433-440.
- Incardona, J. P. and Eaton, S.** (2000). Cholesterol in signal transduction. *Curr. Opin. Cell Biol.* **12**, 193-203.
- Iwabuchi, K., Handa, K. and Hakomori, S.** (1998). Separation of "glycosphingolipid signaling domain" from caveolin-containing membrane fraction in mouse melanoma B16 cells and its role in cell adhesion coupled with signaling. *J. Biol. Chem.* **273**, 33766-33773.
- Johannessen, L. E., Haugen, K. E., Ostvold, A. C., Stang, E. and Madshus, I. H.** (2001). Heterodimerization of the epidermal-growth-factor (EGF) receptor and ErbB2 and the affinity of EGF binding are regulated by different mechanisms. *Biochem. J.* **356**, 87-96.
- Kilsdonk, E. P., Yancey, P. G., Stoudt, G. W., Bangerter, F. W., Johnson, W. J., Phillips, M. C. and Rothblat, G. H.** (1995). Cellular cholesterol efflux mediated by cyclodextrins. *J. Biol. Chem.* **270**, 17250-17256.
- Klein, U., Gimpl, G. and Fahrenholz, F.** (1995). Alteration of the myometrial plasma membrane cholesterol content with beta-cyclodextrin modulates the binding affinity of the oxytocin receptor. *Biochemistry* **34**, 13784-13793.
- Kurzchalia, T. V. and Parton, R. G.** (1999). Membrane microdomains and caveolae. *Curr. Opin. Cell Biol.* **11**, 424-431.
- Liscum, L. and Klensek, J. J.** (1998). Niemann-Pick disease type C. *Curr. Opin. Lipidol.* **9**, 131-135.
- Meuillet, E. J., Kroes, R., Yamamoto, H., Warner, T. G., Ferrari, J., Mania-Farnell, B., George, D., Rebbaa, A., Moskal, J. R. and Bremer, E. G.** (1999). Sialidase gene transfection enhances epidermal growth factor receptor activity in an epidermoid carcinoma cell line, A431. *Cancer Res.* **59**, 234-240.
- Meuillet, E. J., Mania-Farnell, B., George, D., Inokuchi, J. I. and Bremer, E. G.** (2000). Modulation of EGF receptor activity by changes in the GM3 content in a human epidermoid carcinoma cell line, A431. *Exp. Cell Res.* **256**, 74-82.
- Miller, K., Beardmore, J., Kanety, H., Schlessinger, J. and Hopkins, C. R.** (1986). Localization of the epidermal growth factor (EGF) receptor within the endosome of EGF-stimulated epidermoid carcinoma (A431) cells. *J. Cell Biol.* **102**, 500-509.
- Mineo, C., Gill, G. N. and Anderson, R. G.** (1999). Regulated migration of epidermal growth factor receptor from caveolae. *J. Biol. Chem.* **274**, 30636-30643.

- Parton, R. G.** (1994). Ultrastructural localization of gangliosides; GM1 is concentrated in caveolae. *J. Histochem. Cytochem.* **42**, 155-166.
- Pike, L. J. and Casey, L.** (1996). Localization and turnover of phosphatidylinositol 4,5-bisphosphate in caveolin-enriched membrane domains. *J. Biol. Chem.* **271**, 26453-26456.
- Pike, L. J. and Miller, J. M.** (1998). Cholesterol depletion delocalizes phosphatidylinositol bisphosphate and inhibits hormone-stimulated phosphatidylinositol turnover. *J. Biol. Chem.* **273**, 22298-22304.
- Rebbaa, A., Hurh, J., Yamamoto, H., Kersey, D. S. and Bremer, E. G.** (1996). Ganglioside GM3 inhibition of EGF receptor mediated signal transduction. *Glycobiology* **6**, 399-406.
- Ringerike, T., Stang, E., Johannessen, L. E., Sandnes, D., Levy, F. O. and Madshus, I. H.** (1998). High-affinity binding of epidermal growth factor (EGF) to EGF receptor is disrupted by overexpression of mutant dynamin (K44A). *J. Biol. Chem.* **273**, 16639-16642.
- Rodal, S. K., Skretting, G., Garred, O., Vilhardt, F., van Deurs, B. and Sandvig, K.** (1999). Extraction of cholesterol with methyl-beta-cyclodextrin perturbs formation of clathrin-coated endocytic vesicles. *Mol. Biol. Cell* **10**, 961-974.
- Sako, Y., Minoghchi, S. and Yanagida, T.** (2000). Single-molecule imaging of EGFR signalling on the surface of living cells. *Nat. Cell Biol.* **2**, 168-172.
- Simons, K. and Ikonen, E.** (2000). How cells handle cholesterol. *Science* **290**, 1721-1726.
- Simons, K. and Toomre, D.** (2000). Lipid rafts and signal transduction. *Nat. Rev. Mol. Cell Biol.* **1**, 31-39.
- Smart, E. J., Graf, G. A., McNiven, M. A., Sessa, W. C., Engelman, J. A., Scherer, P. E., Okamoto, T. and Lisanti, M. P.** (1999). Caveolins, liquid-ordered domains, and signal transduction. *Mol. Cell Biol.* **19**, 7289-7304.
- Sorkin, A. and Carpenter, G.** (1991). Dimerization of internalized epidermal growth factor receptors. *J. Biol. Chem.* **266**, 23453-23460.
- Stang, E., Johannessen, L. E., Knardal, S. L. and Madshus, I. H.** (2000). Polyubiquitination of the epidermal growth factor receptor occurs at the plasma membrane upon ligand-induced activation. *J. Biol. Chem.* **275**, 13940-13947.
- Suarez Pestana, E., Greiser, U., Sanchez, B., Fernandez, L. E., Lage, A., Perez, R. and Bohmer, F. D.** (1997). Growth inhibition of human lung adenocarcinoma cells by antibodies against epidermal growth factor receptor and by ganglioside GM3: involvement of receptor-directed protein tyrosine phosphatase(s). *Br. J. Cancer* **75**, 213-220.
- Subtil, A., Gaidarov, I., Kobylarz, K., Lampson, M. A., Keen, J. H. and McGraw, T. E.** (1999). Acute cholesterol depletion inhibits clathrin-coated pit budding. *Proc. Natl. Acad. Sci. USA* **96**, 6775-6780.
- Torrisi, M. R., Lotti, L. V., Belleudi, F., Gradini, R., Salcini, A. E., Confalonieri, S., Pelicci, P. G. and Di Fiore, P. P.** (1999). Eps15 is recruited to the plasma membrane upon epidermal growth factor receptor activation and localizes to components of the endocytic pathway during receptor internalization. *Mol. Biol. Cell* **10**, 417-434.
- Van de Vijver, M. J., Kumar, R. and Mendelsohn, J.** (1991). Ligand-induced activation of A431 cell epidermal growth factor receptors occurs primarily by an autocrine pathway that acts upon receptors on the surface rather than intracellularly. *J. Biol. Chem.* **266**, 7503-7508.
- Waugh, M. G., Lawson, D. and Hsuan, J. J.** (1999). Epidermal growth factor receptor activation is localized within low-buoyant density, non-caveolar membrane domains. *Biochem. J.* **337**, 591-597.
- Yeagle, P. L.** (1985). Cholesterol and the cell membrane. *Biochim. Biophys. Acta* **822**, 267-287.